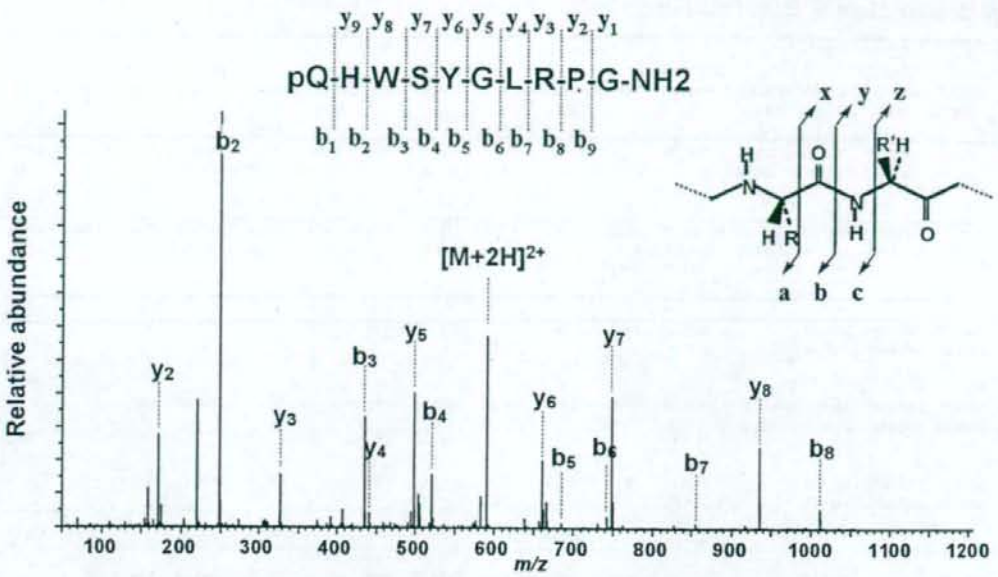

Fig. 2 MS/MS Spectrum of m/z 591.8 (+2) of Gonadrelin

b及びyイオンの集計結果をTable 3に示す．検出されたフラグメントイオンは，装置，測定条件により違いがあったが，生じることが予想されるフラグメントイオン $b_{1\sim9}$ 及び $y_{1\sim9}$ のうち，b_2，b_3，b_4，b_6，b_8，y_2，y_3，y_5，y_6，y_7 及び y_8 が検出されやすい傾向があった．2回の測定とも検出できたイオンの数は，平均13.1個（7～16個）であった．また，各機関において規格として設定可能と判断されたイオンは，平均10.3個（5～16個）であった．各試験室で観測したフラグメントイオンの m/z 値の実測値の理論値からの誤差は，一試験室（E1及びE2）を除くと−0.45～0.22であり，各測定での誤差の平均は−0.21～0.11，また標準偏差は0.001～0.15であった（Table 3）．機関Eにおいて実測値と理論値との差が大きくなった原因として，装置の分解能が低いこと，及びピークがノイズや他のフラグメントイオンと重なった場合にピークがブロードになったことが考えられた．機関Eを除く各試験室（機関Hでは2種類の条件で測定が行われているので，フラグメントイオンが多く観測されたH1の測定値を採用した．）で観測した $b_{2\sim8}$ 及び $y_{2\sim8}$ の各フラグメントイオンの m/z 値の室内再現標準偏差及び室間再現標準偏差を求めたところ，それぞれ0.01～0.11及び0.05～0.14であった（データ非表示）．

還元アルキル化インスリンA鎖 インスリンA鎖のMS/MSによって検出されたb及びyイオンの数をTable 4に示す．CAM化インスリンA鎖を測定した試験室A4及びE1，及びCM化インスリンA鎖を測定した試験室A4，C1，C2及びE1では，前駆イオンのシグナル強度が低く，フラグメントイオンを検出できなかった．MS/MSスペクトルを測定できた試験室においては，13～35個のフラグメントイオンを検出することができた．また，6～26個のフラグメントイオンを規格として設定可能であると判断した．

還元アルキル化インスリンB鎖 いずれの還元アルキル化方法でも，5個以上のフラグメントイオンを検出することができた（Table 4）．また，4～35個のフラグメントイオンを規格として設定可能であると判断した．

4．考　察

本研究では，ペプチド及びたん白質性医薬品の確認試験法として適していると思われるイオン化方法，分析計及び測定方法を設定し，MSを用いた標準的確認試験法を作成した．更に，8機関共同で試験法の適用可能性を検証した．

Molecular Mass at Each Laboratory

E1	E2	G	H	ESI + MALDI				ESI				MALDI			
MALDI TOF	DHB MALDI TOF	MALDI TOF	MALDI TOFTOF	Average	Bias	Standard deviation SRW	SR (ppm)	Average	Bias	Standard deviation SRW	SR (ppm)	Average	Bias	Standard deviation SRW	SR (ppm)
307.04	(307.01)	307.09	307.08	307.08	-0.01	0.0027	0.040	307.08	0.00	0.000	0.045	307.06	-0.02	0.0049	0.027
307.04	(307.01)	307.09	307.09	(n = 13)			131	(n = 9)			147	(n = 4)			88
1181.64	(1181.65)	1181.57	1181.57	1181.57	0.00	0.032	0.058	1181.55	-0.02	0.013	0.054	1181.60	0.02	0.049	0.060
1181.66	(1181.69)	1181.72	1181.57	(n = 13)			49	(n = 8)			46	(n = 5)			51
				1181.7	-0.6										
				(n = 1)											
2802.61	(2802.08)	2802.05		2802.25	0.02	0.007	0.21	2802.21	-0.02			2802.28	0.05		
2802.61	(2802.08)	2802.04		(n = 5)			75								
2609.97	(2609.90)	2609.69	2610.02	2610.09	0.00	0.185	0.20	2610.14	0.05			2610.03	-0.05		
2609.92	(2609.78)	2610.28	2610.12	(n = 8)			75								
2614.27	(2614.03)	2614.89		2614.19	0.17	0.191	0.28	2614.04	0.02			2614.41	0.39		
2614.20	(2614.04)	2614.29		(n = 5)			106								
				2614.7	-1.1										
				(n = 2)											
3638.28		3638.41		3638.00	0.20	0.039	0.30	3637.78	-0.02			3638.14	0.34		
3638.31		3638.29		(n = 5)			82								
	3640.2			3639.8	-0.4										
	3639.4														
3541.77		3542.08	3541.81	3541.75	0.02	0.089	0.16	3541.70	-0.03			3541.79	0.07		
3541.54		3542.01	3541.64	(n = 9)			44								
	3543.4			3543.7	-0.3										
	3544.0														
3544.10		3544.09		3543.94	0.25	0.134	0.23	3543.82	0.13			3544.11	0.41		
3544.05		3544.08		(n = 7)			65								
	3545.4			3545.8	-0.15										
	3545.4			(n = 3)											
			5803.63	5803.91	0.27	0.011	0.54	5803.98	0.34			5803.63	-0.01		
			5803.62	(n = 5)			92	(n = 4)				(n = 1)			
5807.7	(5707.6)	5805.9		5806.5	-1.1	0.43	0.90	5806.7	-0.9			5806.3	-1.3		
5807.7	(5807.6)	5806.0		(n = 9)			155	(n = 5)				(n = 4)			
22118.1		22101.9	22124.8	22118.8	-6.0	2.5	10.5	22124.5	-0.2	0.54	0.92	22108.4	-16.3	4.2	12.2
22117.7		22112.8	22120.6	(n = 14)			476	(n = 9)			42	(n = 5)			552
66405		66357	66419	66418	-20	20	43	66447	10	7.7	20	66382	-55	29	34
66408		66360	66381	(n = 11)			649	(n = 6)			306	(n = 5)			517

は，再現良く十分な強度で検出されたものとした．

グルタチオン　MS/MSにより生じることが予想されるフラグメントイオン b_{1-2} 及び y_{1-2} のうち，IT型分析計を用いたときにローマスカットオフにより低 m/z のイオン（y_1，m/z 76.0）が検出されなかったことを除き，すべてのb及びyイオンが検出された（データ非表示）．

ゴナドレリン　ゴナドレリンのMS/MSスペクトルの例をFig. 2に示す．ペプチドをMS/MSにより断片化したとき，主にペプチド結合の位置で開裂が起こる．生じた断片のうち，N末端を含むフラグメントイオンは，a，b及びc系列，またC末端を含むフラグメントイオンは，x，y及びz系列と呼ばれる[8]．低エネルギー衝突誘起解離やポストソース分解では，主にb及びy系列のフラグメントイオンが生じる．各b及びyイオンが生成する際の切断位置を図中に示した．各機関で測定したゴナドレリンのMS/MSスペクトル上に検出された

Table 2 Summary of Measurement of

Laboratory				A1	A2	A3	B1	B2	C1	C2	C3	D	F	A4	B4
Mass type	Theoretical mass			ESI QTOF	ESI IT	ESI FT-ICR	ESI IT	-ESI TOF	ESI IT	ESI QTOF	ESI TOF	ESI QTOF	ESI OT	MALDI TOFTOF	MALD TOF
Sample	(Da)			Observed mass											
Glutathione	Mmono	307.084	1	307.08	307.17	307.08	307.1	307.05	307.0	307.08		307.09	307.08	307.04	
			2	307.08	307.17	307.08	307.1	307.05	307.0	307.08		307.09	307.08	307.03	
	Mave	307.324	1												
			2												
Gonadrelin	Mmono	1181.573	1	1181.58		1181.58	1181.6	1181.43	1181.5	1181.54		1181.58	1181.57	1181.58	1181.5
			2	1181.57		1181.58	1181.6	1181.43	1181.6	1181.54		1181.58	1181.57	1181.57	1181.5
	Mave	1182.290	1		1181.7										
			2		1181.7										
Human insulin A chain															
Pyridyl ethyl	Mmono	2802.231	1	2802.25								2802.19		2802.18	
			2	2802.25								2802.17		2802.19	
	Mave	2804.249	1												
			2												
Carboxyamidmethyl	Mmono	2610.086	1	2610.11			2610.2	2609.96					2610.08	-	2610.2
			2	2610.11			2610.6	2609.96					2610.08	-	2610.6
	Mave	2611.906	1												
			2												
Carboxymethyl	Mmono	2614.022	1	2614.01		2614.11				-		2614.00		-	
			2	2614.03		2614.11				-		2614.00		-	
	Mave	2615.845	1		2614.6				2615.0						
			2		2614.6				2614.6						
Human insulin B chain															
Pyridyl ethyl	Mmono	3637.800	1	3637.82								3637.74		3637.78	
			2	3637.82								3637.74		3637.79	
	Mave	3640.198	1												
			2												
Carboxyamidmethyl	Mmono	3541.728	1	3541.76			3541.8	3541.51					3541.725	3541.73	3541.8
			2	3541.76			3541.8	3541.51					3541.725	3541.72	3541.8
	Mave	3544.026	1												
			2												
Carboxymethyl	Mmono	3543.696	1	3543.74		3543.80				3543.90		3543.60		3544.14	
			2	3543.72		3544.29				3543.92		3543.60		3544.20	
	Mave	3545.996	1		3546.6				3545.5						
			2		3546.9				3545.4						
Human insulin	Mmono	5803.638	1	5803.60		5803.82					5804.87		5803.65		
			2	5803.59		5803.82					5804.84		5803.65		
	Mave	5807.576	1		5807.0		5807.2	5806.17	5808.2			5805.6		5805.6	5806
			2		5807.0		5807.2	5806.17	5807.0			5805.7		5805.8	5805
Human growth hormone	Mmono	22111.0	1												
			2												
	Mave	22124.8	1	22124.4	22124.3	22125.1	22124	22125	22125.0		22123.0	22124.8	22124.1	22101.4	22097
			2	22124.9	22124.8	22127.1	22124	22125	22124.0		22123.0	22124.8	22124.1	22096.9	22093
Human serum albumin	Mmono	66395	1												
			2												
	Mave	66437	1	66440	66500	-		66439	-		66447	66437	66437	66346	6644
			2	66439	66474	-		66440	-		66440	66438	66436	66346	6635

Upper: monoisotopic mass.
Lower: average mass.
-, Not detected.

偏差は 20 Da，相対標準偏差は 306 ppm であった．一方，MALDI-MS による測定では，実測値は 66,346～66,440 Da，平均は 66,382 Da，理論値からの実測値の平均の誤差は－55 Da，室間再現標準偏差は 34 Da，相対標準偏差は 517 ppm であった．

3.3 試験案（MS/MS）の適用可能性の検証

機関 A(4)，B(3)，C(2)，D(1)，E(2)，F(1) 及び H(1) においてグルタチオン，ゴナドレリン及びインスリン A 鎖及び B 鎖の MS/MS を測定日を変えて 2 回行い，検出された b 及び y イオン[8]と，そのうち，ペプチドの確認試験の際に検出すべきイオンとして設定できると判断されたイオンを集計した．装置の分解能やデータ処理の仕方等によりピークの見え方が異なることから，フラグメントイオンの検出は，質量分析装置付属のソフトウェアにてピークと認識されたものから目視にて他のイオンと重なっているピークやノイズと疑われるピークを除去することにより判定した．規格として設定できるイオン

MSで測定したヒトインスリンのマススペクトルの例をFig. 1に示す．単同位体質量，最大強度質量及び平均質量に相当する m/z の位置を図中に示した．各機関の単同位体質量の実測値は5,803.59～5,804.87Da,平均は5,803.91Da,理論値(5,803.638)からの実測値の平均の誤差は0.27 Da，室間再現標準偏差は0.54 Da，相対標準偏差は92 ppmであった．また，平均質量の実測値は5,805.1～5,808.2 Da，平均は5,806.5 Da，理論値（5,807.576）からの実測値の平均の誤差は－1.1 Da，室間再現標準偏差は0.90 Da，相対標準偏差は155 ppmであった．

ヒト成長ホルモン　全機関がヒト成長ホルモン（分子量22,125）の平均質量を測定した．平均質量の実測値は22,093.0～22,127.1 Da,平均は22,118.8 Da，理論値（22,124.8）からの実測値の平均の誤差は－6.0 Da，室間再現標準偏差は10.5 Da，相対標準偏差は476 ppmであった．なお，ESI-MSによる測定では，実測値は22,123.0～22,127.1 Da，平均は22,124.5 Da，理論値からの実測値の平均の誤差は－0.2 Da，室間再現標準偏差は0.92 Da，相対標準偏差は42 ppmであった．それに対して，MALDI-MSでは，実測値は22,093.0～22,124.8 Da，平均は22,108.4 Da，理論値からの実測値の平均の誤差は-16.3 Da，室間再現標準偏差は12.2 Da，相対標準偏差は552 ppmであった．

ヒト血清アルブミン　全機関がヒト血清アルブミン（分子量66,437）の平均質量を測定した．平均質量の実測値は66,346～66,500 Da,平均は66,418 Da，理論値からの実測値の平均の誤差は－20 Da，室間再現標準偏差は43 Da，相対標準偏差は649 ppmであった．ESI-MSによる測定では，実測値は66,436～66,500 Da，平均は66,447 Da，理論値からの実測値の平均の誤差は10 Da，室間再現標準

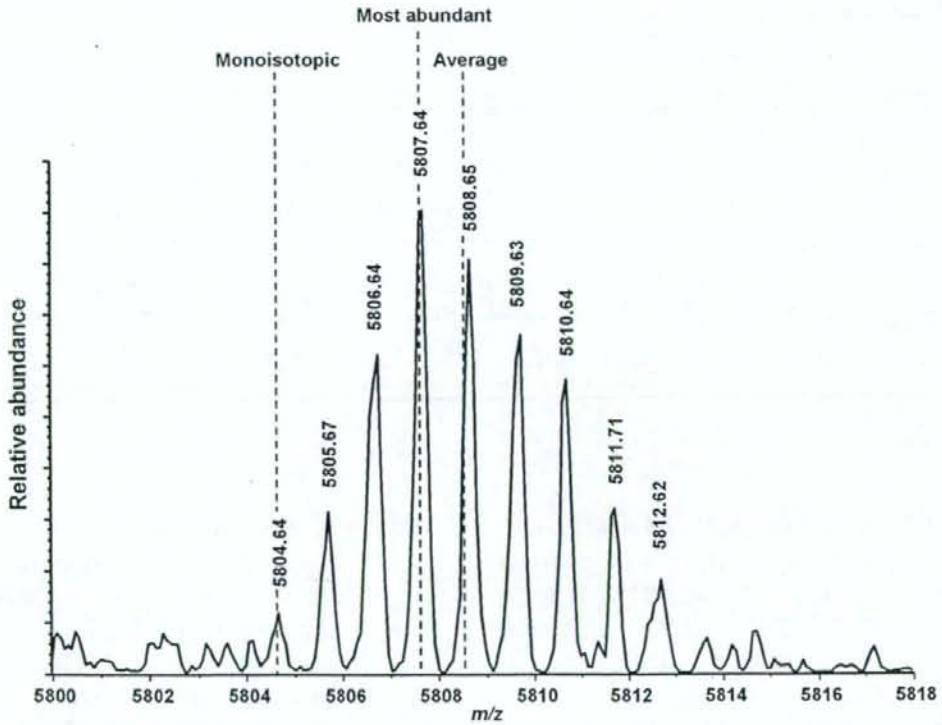

Fig. 1　MALDI-MS Spectrum of Human Insulin
Monoisotopic mass, most abundant mass and average mass were deduced to be 5803.63, 5806.64 and 5807.53, respectively.

2.9 測定機関（試験室数）

国立医薬品食品衛生研究所（4），キリンファーマ㈱（4），中外製薬㈱（3），アステラス製薬㈱（1），大日本住友製薬㈱（1），サーモフィシャーサイエンティフィック㈱（1），近畿大学（1）及び島津製作所㈱（1）

3. 研究結果

3.1 MSを用いたペプチド及びたん白質性医薬品の確認試験法案の作成

標準的試験法として，以下のような測定条件を採用し確認試験法案（別紙1）を作成した．イオン化方法にはESI及びMALDIを使用し，分析計にはQ型，IT型，TOF型又はFT-ICR型等を使用することとした．ESI-MSでは，溶媒として，酢酸，ギ酸又はTFA等を含む水，アセトニトリル及びメタノールの混液等を使用し，試料導入にはインフュージョンやHPLC等を使用することとした．MALDI-MSでは，マトリックスとして，ペプチドにはCHCA又はDHBを，たん白質にはSAを用い，TFAを含む水，アセトニトリル混液に溶解し，試料とマトリックスを混合しサンプルプレート上に乾固し，質量分析に供することとした．質量校正は，装置メーカー推奨のもの，もしくは分子質量が既知の質量分析用標準品，ペプチド及びたん白質を用いるものとした．ジスルフィド結合の還元アルキル化方法には，PE化，CAM化又はCM化を用いることとした．

3.2 試験案（MS）の適用可能性の検証

インスリンは各機関で還元アルキル化を行った．確認試験法案に基づいて，グルタチオン，ゴナドレリン，還元アルキル化インスリンA鎖及びB鎖，インスリン，ヒト成長ホルモン及びヒト血清アルブミンの分子質量を日を変えて2回測定した．各機関で使用した装置，質量校正標準品，試料調製法及び試料導入法をTable 1A及び1Bにまとめた．また，Table 2に各機関で得られた分子質量実測値（上段に単同位体質量の実測値，下段に平均質量の実測値），並びに集計結果を示す．

グルタチオン　すべての機関において，グルタチオン（分子量：307.3）の単同位体質量を測定した．単同位体質量の実測値は307.00～307.17 Da，平均は307.08 Da，理論値（307.084）からの実測値の平均の誤差は−0.01 Da，室間再現標準偏差は0.040 Da，相対標準偏差は131 ppmであった．

ゴナドレリン　1試験室を除いて，ゴナドレリン（分子量1,182.3）の単同位体質量を測定した．単同位体質量の実測値は1,181.43～1,181.72 Da，平均は1,181.57 Da，理論値（1,181.573）からの実測値の平均の誤差は0.00 Da，室間再現標準偏差は0.058 Da，相対標準偏差は49 ppmであった．

還元アルキル化ヒトインスリンA鎖　PE化A鎖（分子量：2,804.2），CAM化A鎖（分子量：2,611.9）及びCM化A鎖（分子量：2,615.8）の測定では，2試験室を除いて単同位体質量を測定した．単同位体質量の実測値は，それぞれ，2,802.04～2,802.61，2,609.69～2,610.60及び2,614.00～2,614.89，平均は2,802.25，2,610.09及び2,614.19であり，理論値（2,802.231，2,610.086及び2,614.022）からの実測値の平均の誤差は0.02，0.00及び0.17 Da，室間再現標準偏差は0.21，0.20及び0.28 Da，相対標準偏差は75，75及び106 ppmであった．PE化インスリンA鎖を測定した5試験室（4機関）は，いずれもプロトン化分子を観測することができた．これに対して，CAM化インスリンA鎖を測定した9試験室（6機関）のうちの1試験室，CM化インスリンA鎖を測定した9試験室（5機関）のうち2試験室で，プロトン化分子を観測できなかった．インスリンA鎖は分子内にシステイン残基を4個含み，還元アルキル化の種類がMSの検出感度に大きく影響することが示された．

還元アルキル化インスリンB鎖　PE化B鎖（分子量：3,640.2），CAM化B鎖（分子量：3,544.0）及びCM化B鎖（分子量：3,546.0）の測定では，12試験室が単同位体質量を，3試験室で平均質量を測定した．単同位体質量の実測値は，それぞれ，3,637.74～3,638.41，3,541.51～3,542.08及び3,543.60～3,544.29，平均は3,638.00，3,541.75及び3,543.94であり，理論値（3,637.800，3,541.728及び3,543.696）からの実測値の平均の誤差は0.20，0.02及び0.25 Da，室間再現標準偏差は0.30，0.16及び0.23 Da，相対標準偏差は82，44及び65 ppmであった．

ヒトインスリン　ヒトインスリン（分子量5,807.6）の測定では，5試験室が単同位体質量を測定し，9試験室が平均質量を測定した．MALDI-

by Individual Laboratories (MALDI)

Human growth hormone	Human serum albumin	Sample introduction methods Matrix solutions and deposition methods			
BSA (S) 16952.27, 39212.28, 66430.09 12.5 μM SA1 Spot1 linear mode	Ald, BSA (S) 39212.28, 66430.09 50 μM SA1 Spot1 linear mode	CHCA1 5 mg/ml 0.1 % TFA/50 % ACN	SA1 5 mg/ml 0.1 % TFA/50 % ACN	Spot1 Deposit 1 μl of mixture of 2 μl of sample sol. and 10 μl of matrix sol.	
TN, ProA, BSA (B) 23982, 44613, 66431 1 mg/ml (45 μM) DDW SA2 Spot3 linear mode	 1 mg/ml (15 μM) DDW SA2 Spot3 linear mode	CHCA2 0.7 mg/ml 2-PrOH:EtOH = 3:1	SA2 Saturated sol. 0.1 % TFA:ACN = 2:1	Spot2 Deposit 1 μl of mixture of 1 μl of sample sol. and 1 μl of matrix sol., then recrystallize	Spot3 Deposit 1 μl of sample sol. and 1 μl of matrix sol.
apoMG, CA (S) 8476.8 (+2), 16952.4, 33904.0 (dimer), 14492.2 (+2), 28983.4 100 μM SA3 Spot5 linear mode	BSA (S) 33216.55 (+2), 66430.09 ~30 μM SA3 Spot5 linear mode	CHCA3 25-30 mg/ml 0.3 % TFA/50 % ACN (10 % EtOH)	DHB1 55-65 mg/ml 0.3 % TFA/50 % ACN (10 % EtOH)	SA3 55-65 mg/ml 0.3 %TFA/50 % ACN (10 % EtOH)	Spot4 Deposit 0.5 μl of matrix sol. and 0.5 μl of sample sol.
CyC, TN (B) 12360.97, 23982 1.0 mg/ml (45 μM) SA4 Spot2 linear mode	Ald, BSA (B) 39212.28, 66430.09 1.0 mg/ml (15 μM) SA4 Spot2 linear mode	CHCA4 10 mg/ml 0.1 % TFA/50 % ACN	SA4 5 mg/ml 0.1 % TFA/50 % ACN		Spot5 Deposit 0.7 μl of mixture of 1 μl of sample sol. and 1 μl of matrix sol.
Ald (S) 19607.64 (+2), 39212.28 10 μM SA4 Spot6 linear mode	BSA (S) 33216.55 (+2), 66430.09 10 μM SA4 Spot6 linear mode	SA4 10 mg/ml 0.1 % TFA/50 % ACN	Spot6 Deposit 1 μl of mixture of 1 μl of sample sol. and 4 μl of matrix sol.		

Ubl: ubiquitin I, CyC: cytochrome C, apoMG: apomyoglobin, CA: carbonic anhydrase, TN: trypsinogen, ProA: protein A, Ald: aldolase, BSA: bovine serum albumin.

2.7 還元アルキル化

2.7.1 還元ピリジルエチル（PE）化

試料約20 μgを6 M塩酸グアニジンを含む0.25 Mトリス緩衝液100 μLに溶かし，1 Mジチオスレイトール溶液約3.5 μL（又は10% 2-メルカプトエタノール溶液約5 μL）を加えた．この液を窒素あるいはアルゴンの存在下で暗所に室温もしくは37℃で1時間放置した後，反応液に4-ビニルピリジン約1 μLを加え，更に1時間室温で暗所に放置した．逆相HPLC，ゲル濾過又は透析等を用いて脱塩した．

2.7.2 還元カルボキシアミドメチル（CAM）化（または還元カルボキシメチル（CM）化）

試料約20 μgを6 M塩酸グアニジンを含む0.25 Mトリス緩衝液20 μLに溶かし，20 mMジチオスレイトール溶液10 μLを加えた．この液を窒素あるいはアルゴンの存在下で暗所に37℃で1時間30分放置した後，7.4 mg/mLのヨードアセタミド溶液（CM化の場合はヨード酢酸溶液）10 μLを加えて更に45分間37℃で暗所に放置した．逆相HPLC，ゲル濾過又は透析等を用いて脱塩した．

2.8 統計処理

各測定は，日を変えて2回行った．分子質量の実測値について，分散分析により室内及び室外再現標準偏差を計算した．同一の研究機関及び同一試験者であっても，タイプの異なる装置を用いた場合は，異なる試験室と見なした．

Table 1B Mass Spectrometers and Methods Used

Laboratory Mass spectrometor Operator	Sample	Glutathione	Gonadrelin	Human insulin A chain	Human insulin B chain	Human insulin
A4 4800 plus (TOFTOF) Applied Biosystems Operator a3	Calibrator[a,b] *m/z*	BK1-7, Angt II, $P_{14}R$, ACTH18-39 (S) 757.400, 1046.542, 1533.858, 2465.199				Ins_B, CyC, apoMG, Ald, BSA 5734.51, 12361.96,
	Sample Conc.[c,d]	25 mM	6.3 mM	25 μM (PE), 100 μM (CAM, CM)		83 μM
	Matrix	CHCA1	CHCA1	CHCA1	CHCA1	SA1
	Deposition method	Spot1	Spot1	Spot1	Spot1	Spot1
	Mode	reflectron mode	reflectron mode	reflectron mode	reflectron mode	linear mode
B4 Autoflex II (TOF) Brucker Daltonics Operator b1	Calibrator[a,b] *m/z*		BK1-7, Angt II, SubP (B) 757.40, 1046.54, 1347.74	ACTH1-17, ACTH18-39, So28 (B) 2093.09, 2465.20, 3147.47		Ins, CyC, apoMG (B) 5734.56, 6181.05, 8476.77
	Sample Conc.[c] Solvent		0.5 mg/ml (0.42 mM) DDW	30 μM ACN:DDW:TFA = 700:300:1	40 μM	0.5 mg/ml (86 μM) DDW
	Matrix		CHCA2	CHCA2	CHCA2	SA2
	Deposition method		Spot2	Spot2	Spot2	Spot3
	Mode		reflectron mode	reflectron mode	reflectron mode	linear mode
	Others		Recrystallizing sol: EtOH:ACN:0.1%TFA = 6:3:1			
E Voyager DE RP (TOF) Applied Biosystems Operator e1	Calibrator[a,b] *m/z*	GRGDTP (S), Angt I (P), ACTH18-39 (S) 601.282, 1295.678, 2464.191				
	Sample Conc.[c,d]	1～10 mM	1～10 μM	1～10 μM	1～10 μM	1～10 μM
	Matrix	CHCA3 (DHB1)	CHCA3 (DHB1)	CHCA3 (DHB1)	CHCA3 (DHB1)	CHCA3 (DHB1)
	Deposition method	Spot4 (Spot5)	Spot4 (Spot5)	Spot4 (Spot5)	Spot4 (Spot5)	Spot4 (Spot5)
	Mode	reflectron mode	reflectron mode	reflectron mode	reflectron mode	reflectron mode
G Voyager DE-PRO (TOF) Applied Biosystems Operator g1	Calibrator[a,b] *m/z*	CHCA, Bom (B) 190.178(+2), 1619.822	Angt II, ACTH18-39 (B) 1046.541, 2465.198	ACTH18-39, So28 (B) 2465.198, 3147.471	ACTH18-39, Ubl (B) 2465.198, 8565.76	Ins_B, Ubl (B) 5734.51, 8565.76
	Sample Conc.[c,d]	1.0 mg/ml (3 mM)	1.0 mg/ml (0.85 mM)	1.0 mg/ml (0.17 mM)	1.0 mg/ml (0.17 mM)	1.0 mg/ml (0.17 mM)
	Matrix	CHCA4	CHCA4	CHCA4	CHCA4	CHCA4
	Deposition method	Spot2	Spot2	Spot2	Spot2	Spot2
	Mode	reflectron mode	reflectron mode	reflectron mode	reflectron mode	reflectron mode
	Others	Recrystallizing sol.: ACN:0.1 % TFA = 1:1				
H AXIMA-TOF[2] (TOFTOF) Shimazu Operator h1	Calibrator[a,b] *m/z*	CHCA 190.050 (+2), 379.093	CHCA, Angt II, Angt I (S) 190.050 (+2), 379.093, 1046.542, 1296.685	CHCA, Angt II, ACTH18-39, ACTH7-38 (S) 190.050 (+2), 379.093, 1046.542, 2465.20,		Ins_H (S) 5803.64
	Sample Conc.[c,d]	0.5 mg/ml (1.6 mM)	0.5 mg/ml (0.42 mM)	10 μM	10 μM	10 μM
	Matrix	CHCA1	CHCA1	CHCA1	CHCA1	CHCA1
	Deposition method	Spot5	Spot5	Spot5	Spot5	Spot5
	Mode	reflectron mode	reflectron mode	reflectron mode	reflectron mode	reflectron mode
	Others			Zip TipC18		

[a]. Angt I: anziotensin I, Bom: bombesin, BK1-7: bradykinin fragment 1-7, Angt II: anziotensin II, SubP: substance P, So28: somatostatin 28, Ins_B: bovine insulin, Ins_H: human insulin.
[b]. Manufacturer, S: Sigma-Aldrich; B: Brucker Daltonics, P: Peptide Institute.
[c]. Estimated values.
[d]. Dissolved in 0.1 % TFA/50 % ACN.

溶液を1：1～5の割合で混合し，マイクロピペットを用いてサンプルプレートに滴下し乾固させた．若しくは，サンプルプレート上で試料溶液とマトリックス溶液を混合し乾固させた．その他に，試料溶液とマトリックス溶液をサンプルプレートに乾固した後，再結晶化を行う手法を用いた．サンプルプレートを質量分析計に設置し，N_2 レーザーを照射して試料をイオン化し，ポジティブイオンモードでマススペクトルを測定した．

2.5.3 MS/MS

MSと同様に試料をイオン化した後，プロトン化分子を前駆イオンとして選択し，適切なフラグメント化の条件を設定し実行した．

2.6 分子質量の計算

観測されたイオンの m/z 値と価数から分子質量を計算した．単同位体ピークが確認できた場合は単同位体質量を計算し，確認できなかった場合はピーク頂点より平均質量を計算した．分子量の大きなたん白質のESI-MSにおいて多数の多価イオンとして観測された場合は，デコンボルーション処理によりたん白質分子の質量を求めた．単同位体質量及び平均質量の理論値は，単同位体精密質量 ^{1}H: 1.007825, ^{12}C: 12.000000, ^{14}N: 14.003074, ^{16}O: 15.994915, ^{32}S: 31.972072[6] 及び原子量 H: 1.00794, C: 12.0107, N: 14.0067, O: 15.9994, S: 32.065[7] を用いて計算した．

by Individual Laboratories (ESI)

Human insulin	Human growth hormone	Human serum albumin	Sample introduction methods
1654.6875, 1790.6623, 1926.6371, 2062.6119 10 μM Tip1 1600 V	10 μM Syr1 (0.3 μl/min) 2400 V Gel filtration	10 μM Syr1 (0.3 μl/min) Gel filtration	Tip1 0.1 % AcOH/50 % MeOH Syr1 0.1 % AcOH/50 % MeOH HPLC1 C8 0.1 % formic acid/2 % ACN 0.1 % formic acid/90 % ACN
10 μM Syr1 (3 μl/min) 2000 V	2 μM Syr1 (3 μl/min) 2000 V Gel filtration	8 μM Syr1 (3 μl/min) 2000 V Gel filtration	Syr2 5 mM $AcONH_4$ (pH 8.5)/50 % MeOH
10 μM Syr1 (3 μl/min) 2000 V	10 pmol HPLC2 (3 μl/min) 2000 V Gel filtratiom	10 pmol HPLC2 (3 μl/min) 2000 V Gel filtratiom	HPLC2 C18 0.1 % formic acid/2 % ACN 0.1 % formic acid/90 % ACN
20 μg (3.4 nmol) HPLC3 (0.2 ml/min) 4000 V	40 μg (1.8 nmol) HPLC3 (0.2 ml/min) 4000 V		HPLC3 C8 0.1 % TFA 0.085 % TFA/47 % ACN
1821.7206, 1971.6149 5 μg (0.86 nmol) HPLC3 (50 μl/min) 3000 V	10 μg (0.45 nmol) HPLC3 (50 μl/min) 3000 V	10 μg (0.15 nmol) HPLC3 (50 μl/min) 3000 V	
10 μM Syr1 (20 μl/min) 4500V	10 μM Syr1 (20 μl/min) 4500V	10 μM Syr1 (20 μl/min) 4500V dialysis	HPLC4 C4 0.1 % TFA/2 % ACN 0.1 % TFA/98 % ACN
1521.9321, 1671.8264, 1821.7206, 1971.6149			
NaI 10 μM Syr1 (5 μl/min) 3000V	10 μM Syr1 (5 μl/min) 3000V	10 μM Syr1 (5 μl/min) 3000V dialysis	
785.8 5 μg (0.86 nmol) HPLC5 (0.25 ml/min) 5000 V	125 ng (5.6 pmol) HPLC5 (0.25 ml/min) 5000 V	63 ng (0.94 pmol) HPLC5 (0.25 ml/min) 5000 V	HPLC5 C4 0.1 % formic acid 1.0 % formic acid/ACN
1 μM Syr3 (5 μl/min) 2000V	1 pmol HPLC6 (3 μl/min) 2000V	1 pmol HPLC6 (3 μl/min) 2000V	Syr3 0.1 % formic acid/50 % AC HPLC6 C18 0.1 % formic acid 0.1 % formic acid/ACN

Table 1A Mass Spectrometers and Methods Used

Laboratory Mass spectrometer Operator	Sample Method	Glutathione	Gonadrelin	Human insulin A chain		Human insulin B cha
A1	Calibrator	YOKUDELNA (JEOL)				
Qstar Elite (QTOF)	*m/z*	158.9646, 294.9394, 430.9142, 566.8890, 702.8638, 838.8386, 974.8134, 1110.7882, 1246.7630, 1382.7379, 1518.7127,				
Applied Biosystems	Conc. or amount of sample[a]	5 μM	5 μM	20 μM	20 pmol	20 μM
Operator a1	Sample introduction[b] (flow rate)	Tip1	Tip1	Syr1 (0.3 μl/min)	HPLC1 (0.5 μl/min)	Syr1 (0.3 μl/min)
	Ion spray voltage	1600 V	1600 V	2400 V		2400 V
	Others			PE, CAM	CM	
				Solid-phase extraction using HLB (Waters)		
A2	Calibrator	Caffeine (Sigma-Aldrich), MRFA (Research Plus), Ultramark1621 (Alfa Aesar)				
LTQ (IT)	*m/z*	195.0877, 524.2650, 1121.9970, 1221.9906, 1321.9842, 1421.9779, 1521.9715, 1621.9651, 1721.9587				
Thermo Fisher Scientific	Conc. or amount of sample[a]	5 μM	5 μM	10 μM		10 μM
	Sample introduction[b] (flow rate)	Syr1 (3 μl/min)	Syr1 (3 μl/min)	Syr2 (3 μl/min)		Syr2 (3 μl/min)
Operator a2	Ion spray voltage	2000 V	2000 V	2000 V		2000 V
	Others			Solid-phase extraction using HLB (Waters)		
A3	Calibrator	Caffeine (Sigma-Aldrich), MRFA (Research Plus), Ultramark1621 (Alfa Aesar)				
LTQ FT (FT-ICR)	Conc. or amount of sample[a]	5 μM	5 μM	10 μM		10 μM
Thermo Fisher Scientific	Sample introduction[b] (flow rate)	Syr1 (3 μl/min)	Syr1 (3 μl/min)	Syr2 (3 μl/min)		Syr2 (3 μl/min)
	Ion spray voltage	2000 V	2000 V	2000 V		2000 V
Operator a2	Others			Solid-phase extraction using HLB (Waters)		
B1	Calibrator	ES Tuning Mix Pos (Agilent Technologies)				
Esquire HCT plus (IT)	*m/z*	118.09, 322.05, 622.03, 922.01, 1521.97, 2121.93, 2721.89				
Bruker Daltonics	Conc. or amount of sample[a]	20 μg (65 nmol)	20 μg (17 nmol)	3.1 nmol		3.1 nmol
Operator b1	Sample introduction[b] (flow rate)	HPLC3 (0.2 ml/min)	HPLC3 (0.2 ml/min)	HPLC3 (0.2 ml/min)		HPLC3 (0.2 ml/min
	Ion spray voltage	4000 V	4000 V	4000 V		4000 V
B2	Calibrator	NaI				
LCT (TOF)	*m/z*	322.7782, 472.6725, 622.5667, 772.4610, 922.3552, 1072.2494, 1222.1437, 1372.0379, 1521.9321, 1671.8264,				
Waters	Conc. or amount of sample[a]	5 μg (16 nmol)	5 μg (4.2 nmol)	0.8 nmol		0.8 nmol
Operator b1	Sample introduction[b] (flow rate)	HPLC3 (50 μl/min)	HPLC3 (50 μl/min)	HPLC3 (50 μl/min)		HPLC3 (50 μl/min)
	Ion spray voltage	3000 V	3000 V	3000 V		3000 V
B3	Calibrator	Caffeine (Sigma-Aldrich), MRFA (Research Plus), Ultramark1621 (Alfa Aesar)				
LCQ Advantage MAX	*m/z*	195.0877, 524.2650, 1221.9906, 1521.9715, 1821.9530				
(IT) Thermo Fisher	Conc. or amount of sample[a]	20 μg (65 nmol)	20 μg (17 nmol)	3.1 nmol		3.1 nmol
Scientific	Sample introduction[b] (flow rate)	HPLC3 (0.2 ml/min)	HPLC3 (0.2 ml/min)	HPLC3 (0.2 ml/min)		HPLC3 (0.2 ml/min
Operator b1	Ion spray voltage	5000 V	5000 V	5000 V		5000 V
C1	Calibrator	Caffeine (Sigma-Aldrich), MRFA (Research Plus), Ultramark1621 (Alfa Aesar)				
LCQ Deca (IT)	*m/z*	195.0877, 524.2650, 1221.9906, 1521.9715, 1821.9530				
Thermo Fisher Scientific	Conc. or amount of sample[a]	10 μM	10 μM	4.3 nmol	10 μM	10 μM
	Sample introduction[b] (flow rate)	Syr1 (10 μl/min)	Syr1 (10 μl/min)	HPLC4 (0.5 mL/min)	Syr1 (10 μl/min)	Syr1 (10 μl/min)
Operator c1	Ion spray voltage	5000V	5000V	5000V	5000V	5000V
	Others				purification by RP-HPLC	
C2	Calibrator	NaI				
Ultima API (QTOF)	*m/z*	22.9898, 132.9054, 172.8840, 322.7782, 472.6725, 622.5667, 772.4610, 922.3552, 1072.2494, 1222.1437, 1372.0379,				
Micromass	Conc. or amount of sample[a]	1 μM	10 μM	10 μM		10 μM
Operator c2	Sample introduction[b] (flow rate)	Syr1 (5 μl/min)	Syr1 (5 μl/min)	Syr1 (5 μl/min)		Syr1 (5 μl/min)
	Ion spray voltage	2500V	3000V	3000V		3000V
	Others			purification by RP-HPLC		
C3	Calibrator					
LCT (TOF)	Conc. or amount of sample[a]					
Waters	Sample introduction[b] (flow rate)					
Operator c1	Ion spray voltage					
	Others					
D	Calibrator	NaICs, Glu-fiberinopeptide				
Synapt HDMS	*m/z*	158.9, 228.9, 362.8, 430.8, 498.8, 566.7, 634.7, 702.7, 770.7, 838.7, 906.7, 974.6, 1042.6, 1110.6, 1314.5, 1382.5, 1450.5				
(QTOF) Waters	Conc. or amount of sample[a]	5 μg (16 nmol)	5 μg (4.2 nmol)	0.86 nmol		0.86 nmol
Operator d1	Sample introduction[b] (flow rate)	HPLC5 (0.25 ml/min)	HPLC5 (0.25 ml/min)	HPLC5 (0.25 ml/min)		HPLC5 (0.25 ml/mi
	Ion spray voltage	5000 V	5000 V	5000 V		5000 V
F	Calibrator	Caffeine (Sigma-Aldrich), MRFA (Research Plus), Ultramark1621 (Alfa Aesar)				
LTQ Orbitrap XL (OT)	*m/z*	195.0877, 524.2650, 1121.9970, 1221.9906, 1321.9842, 1421.9779, 1521.9715, 1621.9651, 1721.9587				
Thermo Fisher Scientific	Conc. or amount of sample[a]	1 μM	1 μM	1 μM		1 μM
	Sample introduction[b] (flow rate)	Syr3 (5 μl/min)	Syr3 (5 μl/min)	Syr3 (5 μl/min)		Syr3 (5 μl/min)
Operator f1	Ion spray voltage	2000V	2000V	2000 V		2000V

[a]. Estimated values.

[b]. Tip: tip-based infusion, Syr: syringe infusion.

66,437）を用いた．試料はすべて機関Aが入手し，機関B，C，D，E，F，G及びHに配付した．グルタチオンはペプチド研究所より購入し，秤量後配付した．ゴナドレリン（ゴナドレリン酢酸塩標準品）は財団法人日本公定書協会より供与され，秤量後配付した．ヒトインスリン（ヒューマリンR注）は日本イーライリリー㈱より購入し，分注後配付した．ヒト成長ホルモン（グロウジェクトBC）は大日本住友製薬㈱製を購入し，ゲルろ過により脱塩後分注し，凍結乾燥後配付した．ヒト血清アルブミンはバイオチェイン㈱より購入し，蒸留水に溶解後分注し，凍結乾燥後配付した．

2.2 装　置

ESI-MS装置として，TOF型：LCT（ウォーターズ㈱），Q-TOF型：Qstar Elite（アプライドバイオシステムズ㈱），Ultima API及びSynapt HD-MS（ウォーターズ㈱），IT型：LCQ Deca，LCQ Advantage MAX及びLTQ（サーモフィッシャーサイエンティフィック㈱），Esquire HCT plus（ブルカー・ダルトニクス㈱），オービトラップ（OT）型：LTQ-Orbitrap XL（サーモフィッシャーサイエンティフィック㈱），FT-ICR型：LTQ-FT（サーモフィッシャーサイエンティフィック㈱）を使用した．MALDI-MS装置として，TOF型：Voyager DE RP及びVoyager DE-PRO（アプライドバイオシステムズ㈱），Autoflex II（ブルカー・ダルトニクス㈱），TOFTOF型：4800 plus（アプライドバイオシステムズ㈱），AXIMA-TOF^2（島津製作所㈱）を使用した．

2.3 質量校正

各試験室においてTable 1A及び1Bに示す質量校正標準品を用いて質量校正を行った．ESI-MS装置を使用した場合は，YOKUDELNA，Caffeine＋MRFA＋Ultramark 1621，ヨウ化ナトリウム，ヨウ化ナトリウム・セシウム又はES tuning Mix Pos＋Glu-fibrinopeptideを使用した．MALDI-MS装置を使用した場合は，α-シアノ-4-ヒドロキシ桂皮酸（CHCA），GRGDTP，angiotensin I，ACTH 18-39，bombesin，bradykinin fragment 1-7，angiotensin II，substance P，$P_{14}R$，ACTH 1-17，somatostatin 28，bovine insulin，human insulin，ubiquitin I，cytochrome C，apomyoglobin，carbonic anhydrase，trypsinogen，protein A，aldolase及びbovine serum albumin（BSA）を試料に応じて使用した．質量校正標準品は各機関にて用意した．

2.4 システム適合性

システム適合性は，MSにおいては，「angiotensin Iを測定したとき，そのモノアイソトピック質量が1,295.5～1,295.9である」等により判定した．MS/MSにおいては，「angiotensin Iにつき，上記の条件で操作するとき，b_2^{1+}，b_4^{1+}，b_6^{1+}，y_2^{1+}及びy_4^{1+}のプロダクトイオンが検出される」や「angiotensin Iのm/z＝1,296.7を前駆イオンとしてPSDによる測定を行ったとき，m/z 255.1，269.2，354.2，506.3，513.3，517.2，534.3，619.4，756.4及び1,183.6のうち少なくとも5個のフラグメントイオンが観測される」等により判定した．

2.5 測定方法

2.5.1 ESI-MS

各機関で用いたESI-MSの測定方法をTable 1Aに示した．脱塩した試料を，0.1%酢酸を含むメタノール/水（1：1）混液，5 mM酢酸アンモニウム（pH 8.5）を含むアセトニトリル/水（1：1）混液又は0.1％ギ酸を含むアセトニトリル/水（1：1）混液に溶かし，1～20 μmol/Lの溶液を作成した．試料溶液をESIチップに導入し，電圧をかけてイオン化した後，ポジティブイオンモードでマススペクトルを測定した．もしくは，0.1～1%のギ酸又は0.085～0.1%のトリフルオロ酢酸（TFA）を含む水/アセトニトリル混液を溶離液に用いたHPLCにより試料を分離し，溶出液を直接ESIチップに導入して質量を測定した．

2.5.2 MALDI-MS

各機関で用いたMALDI-MSの測定方法をTable 1Bに示した．試料を水，0.1% TFA又は0.1% TFAを含むアセトニトリル/水（7：3）混液に溶かし，1 μmol/Lから25 mmol/Lの溶液を作成した．マトリックスには，ペプチド試料ではCHCA又は2,5-ジヒドロキシ安息香酸（DHB）を，たん白質試料ではシナピン酸（SA）を使用した．マトリックスは，0.1% TFAを含むアセトニトリル/水（1：1）混液に溶かし，5～10 mg/mLの溶液もしくは飽和溶液とした．又は0.3% TFAを含むアセトニトリル/水（1：1）混液に加温し溶かし，過飽和溶液（CHCA 25～30 mg/mL，DHB及びSA 55～60 mg/mL）とした．試料溶液とマトリックス

1. 緒　言

質量分析(MS)及びタンデム質量分析(MS/MS)は，それぞれ，ペプチドや分子量十万程度までのたん白質の質量を測定できること及びアミノ酸配列に関する情報を得られることから[1~5]，近年，ペプチド及びたん白質性医薬品の特性・構造解析に汎用され，更に確認試験として取り入れられるようになってきた．しかし，ペプチドやたん白質の質量分析において，イオン化法として主にエレクトロスプレーイオン化法（ESI）及びマトリックス支援レーザー脱離イオン化法（MALDI）の2種類が用いられていること，分析計として四重極（Q）型，イオントラップ（IT）型，飛行時間（TOF）型，フーリエ変換イオンサイクロトロン共鳴（FT-ICR）型など複数の装置が用いられていること，装置メーカーごとに推奨している質量校正用標準品が異なっていること，試験者によって分析条件が大きく異なることから，試験結果の許容範囲や試験法としての応用可能性が明確にされていない．そのため，MSやMS/MSを確認試験として広く適用していくには，条件設定をしていく必要があり，装置に依存しないMSを用いた確認試験法の整備と，適用可能性の範囲を明らかにすることが望まれている．そこで，本研究では，国立医薬品食品衛生研究所，バイオ医薬品開発メーカー，大学，MS装置開発メーカーによって，MSを用いたペプチド及びたん白質性医薬品の標準的な確認試験法を作成し，そのバイオ医薬品への適用について検討した．

2. 研究方法

2.1 試　料

グルタチオン（$C_{10}H_{17}N_3O_6S_1$：単同位体質量307.084，平均質量307.3），ゴナドレリン（$C_{55}H_{75}N_{17}O_{13}$：単同位体質量1,181.573，平均質量1,182.3），遺伝子組換えヒトインスリン（$C_{257}H_{383}N_{65}O_{77}S_6$：単同位体質量5,803.638，平均質量5,807.6），遺伝子組換えヒト成長ホルモン（$C_{990}H_{1,528}N_{262}O_{300}S_7$：単同位体質量22,111，平均質量22,125），及び遺伝子組換えヒト血清アルブミン（$C_{2,936}H_{4,590}N_{786}O_{889}S_{41}$：単同位体質量66,395，平均質量

*1 国立医薬品食品衛生研究所生物薬品部　東京都世田谷区上用賀1-18-1（〒158-8501）
Division of Biological Chemistry and Biologicals, National Institute of Health Sciences. 1-18-1, Kamiyoga, Setagaya-ku, Tokyo 158-8501, Japan
*2 キリンファーマ㈱製造本部　群馬県高崎市萩原町100-1（〒370-0013）
Production Division, Kirin Pharma Co., Ltd. 100-1, Hagiwara-machi, Takasaki City, Gunma 370-0013, Japan
*3 中外製薬㈱分析技術研究部　東京都北区浮間5-5-1（〒115-8543）
Analytical Technology Research Department, Chugai Pharmaceutical Co., Ltd. 5-5-1 Ukima, Kita-ku, Tokyo 115-8543, Japan
*4 アステラス製薬㈱製剤研究所　静岡県焼津市大住180（〒435-0072）
Pharmaceutical Analysis, Pharmaceutical Research & Technology Laboratories., Astellas Pharma Inc. 180, Ozumi, Yaizu-shi, Shizuoka 425-0072, Japan
*5 大日本住友製薬㈱技術研究センター分析研究部　大阪府茨木市蔵垣内1-3-45（〒567-0878）
Technology Research and Development Center, Dainippon Sumitomo Pharma Co., Ltd. 1-3-45 Kurakakiuchi, Ibaraki City, Osaka 567-0878
*6 サーモフッシャーサイエンティフィック㈱　神奈川県横浜市神奈川区守屋町3-9 C-2F（〒221-0022）
Chromatography & MS Sales Deptertment, Product marketing Group, Thermo Fisher Scientific K.K TBAJ. 3-9 C-2F, Moriya-cho, Yokohama City, Kanagawa 221-0022, Japan
*7 近畿大学薬学部　大阪府東大阪市小若江3-4-1（〒577-8502）
School of Pharmacy, Kinki University, Kowakae 3-4-1, Higashi-osaka 577-8502, Japan
*8 島津製作所㈱分析計測事業部応用技術部京都アプリケーション開発センター　京都府京都市中京区西ノ京桑原町1（〒604-8511）
Applications Development Center, Analytical Applications Department, Analytical & Measuring Instruments Division, Shimadzu Co. 1 Nishinokyo-Kuwabaracho, Nakagyo-ku, Kyoto 604-8511, Japan
Corresponding author: Nana Kawasaki, Division of Biological Chemistry and Biologicals, National Institute of Health Sciences. 1-18-1, Kamiyoga, Setagaya-ku, Tokyo 158-8501, Japan
E-mail: nana@nihs.go.jp

医薬品研究
Pharm. Regul. Sci.
39(10)627～646(2008)

——資　料——

質量分析を用いたペプチド及びたん白質性医薬品の確認試験法に関する研究**

原園　景*1, 川崎　ナナ*1, 伊藤さつき*1, 小林　哲*1, 石川　リカ*2,
高井　俊紀*2, 古賀　明子*3, 岡本寿美子*3, 山口　秀人*4, 濱詰　康樹*5,
佐藤　貴之*5, 窪田　雅之*6, 掛樋　一晃*7, 木下　充弘*7, 島　圭介*8,
山田　真希*8, 山口　照英*1

(受付：平成20年5月22日，受理：平成20年9月16日)

Study of Mass Spectrometry as an Identification Test for Peptide/Protein Products

Akira HARAZONO*1, Nana KAWASAKI*1, Satsuki ITOH*1, Tetsu KOBAYASHI*1,
Rika ISHIKAWA*2, Toshiki TAKAI*2, Akiko KOGA*3, Sumiko OKAMOTO*3,
Hideto YAMAGUCHI*4, Yasuki HAMAZUME*5, Takayuki SATOH*5,
Masayuki KUBOTA*6, Kazuaki KAKEHI*7, Mitsuhiro KINOSHITA*7,
Keisuke SHIMA*8, Masaki YAMADA*8 and Teruhide YAMAGUCHI*1

Summary

Since mass spectrometry (MS) and tandem mass spectrometry (MS/MS) make it possible to measure accurately the mass of peptides and proteins and provide structural information, they have been used for not only analysis of primary structure and post-translational modification but also identification tests of peptide and protein products. However, assay methods for identification tests have not been fully standardized due to the availability of different ionization methods, many types of analyzers and various analytical conditions. In this paper, mass spectrometry for identification tests of peptide and protein products has been standardized and validated in a collaborative study using several types of mass spectrometers equipped with ESI or MALDI sources. Based on the results of molecular mass measurement from the collaborative study, we propose the following acceptance criteria: i) 0.3 Da (monoisotopic mass) for peptides with masses of <1,000 Da, ii) 300 ppm (monoisotopic mass) and 500 ppm (average mass) for peptides with masses of 1,000～6,000 by ESI-MS and MALDI-MS, and iii) 500 ppm and 1,600 ppm (average mass) for proteins with masses of 6,000～22,000 Da by ESI-MS and MALDI-MS, respectively. Although peptides with masses of 1,000～4,000 Da yielded 5～10 b- and y- series fragments by CID-MS/MS and PSD, the detected ions were not identical among laboratories. Further study is necessary for optimization and standardization of MS/MS conditions.

Key words

Mass spectrometry, Tandem mass spectrometry, Peptide, Protein, Biologicals, Identification test

10. Peggs, K.S., Verfuerth, S., Pizzey, A., Khan, N., Guiver, M., Moss, P.A., and Mackinnon, S. Adoptive cellular therapy for early cytomegalovirus infection after allogeneic stem-cell transplantation with virus-specific T-cell lines. *Lancet* **362**, 1375–1377
11. Dazzi, F., van Laar, J.M., Cope, A., and Tyndall, A. (2007) Cell therapy for autoimmune diseases. *Arthritis Res. Ther.* **9**, 206–214
12. Ringdén, Ö., Uzunel, M., Rasmusson, I., Remberger, M., Sundberg, B., Lönnies, H., Marschall, H.-U., Dlugosz, A., Szakos, A., Hassan, Z., Omazic, B., Aschan, J., Barkholt, L., and Le Blanc, K. (2006) Mesenchymal stem cells for treatment of therapy-resistant graft-versus-host disease. *Transplantation* **81**, 1390–1397
13. Derfoul, A., Perkins, G.L., Hall, D.J., and Tuan, R.S. (2006) Glucocorticoids promote chondrogenic differentiation of adult human mesenchymal stem cells by enhancing expression of cartilage extracellular matrix genes. *Stem Cells* **24**, 1487–1495
14. Nuttelman, C.R., Tripodi, M.C., and Anseth, K.S. (2004) *In vitro* osteogenic differentiation of human mesenchymal stem cells photoencapsulated in PEG hydrogels. *J. Biomed. Mater. Res. A* **68**, 773–782
15. Kulterer, B., Friedl, G., Jandrositz, A., Sanchez-Cabo, F., Prokesch, A., Paar, C., Scheideler, M., Windhager, R., Preisegger, K.-H., and Trajanoski, Z. (2007) Gene expression profiling of human mesenchymal stem cells derived from bone marrow during expansion and osteoblast differentiation. *BMC Genomics* **8**, 70–84
16. Pittenger, M.F., Mackay, A.M., Beck, S.C., Jaiswal, R.K., Douglas, R., Mosca, J.D., Moorman, M.A., Simonetti, D.W., Craig, S., and Marshak, D.R. (1999) Multilineage potential of adult human mesenchymal stem cells. *Science* **284**, 143–147
17. Barrett, T., Troup, D.B., Wilhite, S.E., Ledoux, P., Rudnev, D., Evangelista, C., Kim, I.F., Soboleva, A., Tomashevsky, M., and Edgar, R. (2007) NCBI GEO: mining tens of millions of expression profiles-database and tools update. *Nucleic Acids Res.* **35**, D760–D765
18. Edgar, R., Domrachev, M., and Lash, A.E. (2002) Gene Expression Omnibus: NCBI gene expression and hybridization array data repository. *Nucleic Acids Res.* **30**, 207–210
19. Toda, K., Ishida, S., Nakata, K., Matsuda, R., Shigemoto-Mogami, Y., Fujishita, K., Ozawa, S., Sawada, J., Inoue, K., Shudo, K., and Hayashi, Y. (2003) Test of significant differences with a priori probability in microarray experiments. *Anal. Sci.* **19**, 1529–1535
20. Benini, S., Perbal, B., Zambelli, D., Colombo, M.P., Manara, M.C., Serra, M., Parenza, M., Martinez, V., Picci, P., and Scotlandi, K. (2005) In Ewing's sarcoma CCN3(NOV) inhibits proliferation while promoting migration and invasion of the same cell type. *Oncogene* **24**, 4349–4361
21. Heymans, S., Lupu, F., Terclavers, S., Vanwetswinkel, B., Herbert, J.-M., Baker, A., Collen, D., Carmeliet, P., and Moons, L. (2005) Loss or inhibition of uPA or MMP-9 attenuates LV remodeling and dysfunction after acute pressure overload in mice. *Am. J. Pathol.* **166**, 15–25
22. Mundlos, S., Otto, F., Mundlos, C., Mulliken, J.B., Aylsworth, A.S., Albright, S., Lindhout, D., Cole, W.G., Henn, W., Knoll, J.H.M., Owen, M.J., Mertelsmann, R., Zabel, B.U., and Olsen, B.R. (1997) Mutaions involving the transcription factor CBFA1 cause cleidocranial dysplasia. *Cell* **89**, 773–779
23. Yamamura, Y., Lee, W.L., Inoue, K., Ida, H., and Ito, Y. (2006) RUNX3 cooperates with FoxO3a to induce apoptosis in gastric cancer cells. *J. Biol. Chem.* **281**, 5267–5276
24. Hu, B., Wang, S., Zhang, Y., Feghali, C.A., Dingman, J.R., and Wright, T.M. (2003) A nuclear target for interleukin-1α: Interaction with the growth suppressor necdin modulates proliferation and collagen expression. *Proc. Natl. Acad. Sci. USA* **100**, 10008–10013
25. Chen, C.-J., Kono, H., Golenbock, D., Reed, G., Akira, S., and Rock, K.L. (2007) Identification of a key pathway required for the sterile inflammatory response triggered by dying cells. *Nat. Med.* **13**, 851–856
26. Wan, D., Gong, Y., Qin, W., Zhang, P., Li, J., Wei, L., Zhou, X., Li, H., Qiu, X., Zhong, F., He, L., Yu, J., Yao, G., Jiang, H., Qian, L., Yu, Y., Shu, H., Chen, X., Xu, H., Guo, M., Pan, Z., Chen, Y., Ge, C., Yang, S., and Gu, J. (2004) Large-scale cDNA transfection screening for genes related to cancer development and progression. *Proc. Natl. Acad. Sci. USA* **101**, 15724–15729
27. Herath, N.I., Spanevello, M.D., Sabesan, S., Newton, T., Cummings, M., Duffy, S., Lincoln, D., Boyle, G., Parsons, P.G., and Boyd, A.W. (2006) Over-expression of Eph and ephrin genes in advanced ovarian cancer: ephrin gene expression correlates with shortened survival. *BMC Cancer* **6**, 144–150
28. Woelfle, U., Cloos, J., Sauter, G., Riethdorf, L., Jänicke, F., van Diest, P., Brakenhoff, R., and Pantel, K. (2003) Molecular signature associated with bone marrow micrometastasis in human breast cancer. *Cancer Res.* **63**, 5679–5684
29. Lin, C.G., Chen, C.-C., Leu, S.-J., Grzeszkiewicz, T.M., and Lau, L.F. (2005) Integrin-dependent functions of the angiogenic inducer NOV (CCN3). *J. Biol. Chem.* **280**, 8229–8237
30. Huang, Y., Haraguchi, M., Lawrence, D.A., Border, W.A., Yu, L., and Noble, N.A. (2003) A mutant, noninhibitory plasminogen activator inhibitor type 1 decreases matrix accumulation in experimental glomerulonephritis. *J. Clin. Invest.* **112**, 379–388
31. Sakamoto, K., Yamaguchi, S., Ando, R., Miyawaki, A., Kabasawa, Y., Takagi, M., Li, C.L., Perbal, B., and Katsube, K. (2002) The nephroblastoma overexpressed gene (NOV/ccn3) protein associates with Notch1 extracellular domain and inhibits myoblast differentiation via Notch signalling pathway. *J. Biol. Chem.* **277**, 29399–29405
32. Scherberich, A., Galli, R., Jaquiery, C., Farhadi, J., and Martin, I. (2007) 3D perfusion culture of human adipose tissue-derived endothelial and osteoblastic progenitors generates osteogenic constructs with intrinsic vascularization capacity. *Stem Cells* **25**, 1823–1829

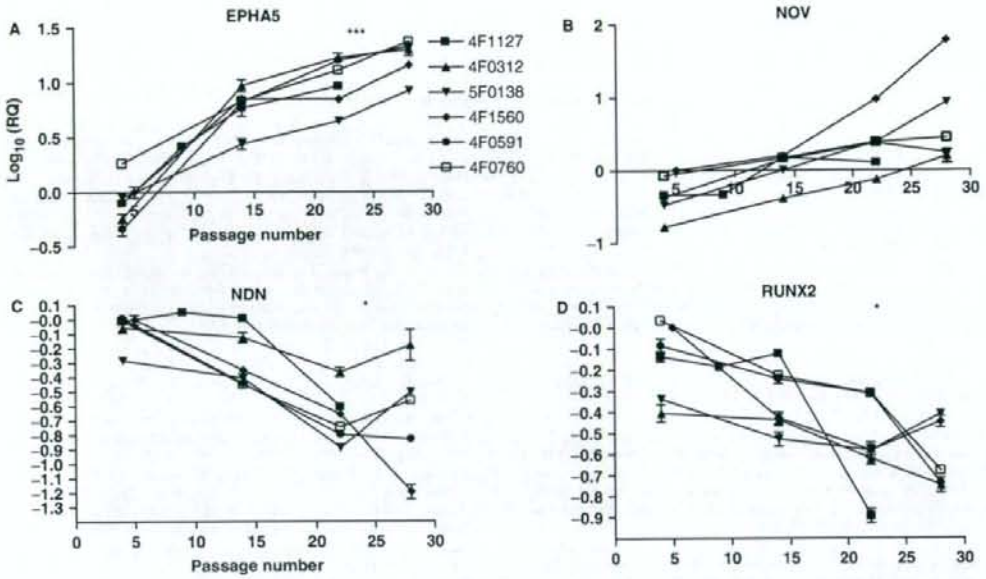

Fig. 4. **Gene expression profiles of culture stage markers suggested for hMSCs.** Individual plots for six batches of hMSCs obtained from RT–PCR data. The expression of *EPHA5* (A), and *NOV* (B) increased, while that of *NDN* (C) and *RUNX2* (D) decreased as the cells were further passaged in each batch. Relative quantity value was plotted on a log 10 scale. The expression of four genes (A–D) was correlated with passage numbers ($P < 0.01$). *** $P < 0.001$, * $P < 0.05$ when the expression in passage #14 was compared to that in late stage (passage #22 and #28) ($n = 6$ in passage #14, $n = 10$ in late stage).

Supplementary data are available at *JB* online.

We thank Dr Y. Hayashi for advice in microarray statistics analysis, and Dr Y. Shinozaki for assistance in microarray experiments. We are also thankful to Dr Y. Ohno and Dr E. Uchida for their support and valuable comments. We are most grateful to C. Aoyagi for her excellent skill in making paraffin sections. This work was supported in part by grants and the Grant-in-Aid for Cancer Research from the Ministry of Health, Labour and Welfare.

REFERENCES

1. Clevers, H. (2005) Stem cells, asymmetric division and cancer. *Nat. Genet.* **37**, 1027–1028
2. Takahashi, K., Tanabe, T., Ohnuki, M., Narita, M., Ichisaka, T., Tomoda, K., and Yamanaka, S. (2007) Induction of pluripotent stem cells from adult human fibroblasts by defined factors. *Cell* **131**, 861–872
3. Fazel, S., Cimini, M., Chen, L., Li, S., Angoulvant, D., Fedak, P., Verma, S., Weisel, R.D., Keating, A., and Li, R.K. (2006) Cardioprotective c-kit+ cells are from the bone marrow and regulate the myocardial balance of angiogenic cytokines. *J. Clin. Invest.* **116**, 1885–1877
4. Rosenzweig, A. (2006) Cardiac cell therapy-mixed results from mixed cells. *N. Engl. J. Med.* **355**, 1274–1277
5. Wollert, K.C., Meyer, G.P., Lotz, J., Lichtenberg, S.R., Lippolt, P., Breidenbach, C., Fichtner, S., Korte, T., Hornig, B., Messinger, D., Arseniev, L., Hertenstein, B., Ganser, A., and Drexler, H. (2004) Intracoronary autologous bone-marrow cell transfer after myocardial infarction: the BOOST randomised controlled clinical trial. *Lancet* **364**, 141–148
6. Schächinger, V., Erbs, S., Elsässer, A., Haberbosch, W., Hambrecht, R., Hölschermann, H., Yu, J., Corti, R., Mathey, D.G., Hamm, C.W., Suselbeck, T., Assmus, B., Tonn, T., Dimmeler, S., and Zeiher, A.M. (2006) Intracoronary bone marrow-derived progenitor cells in acute myocardial infarction. *N. Engl. J. Med.* **355**, 1210–1221
7. Assmus, B., Honold, J., Schächinger, V., Britten, M.B., Fischer-Rasokat, U., Lehmann, R., Teupe, C., Pistorius, K., Martin, H., Abolmaali, N.D., Tonn, T., Dimmeler, S., and Zeiher, A.M. (2006) Transcoronary transplantation of progenitor cells after myocardial infarction. *N. Engl. J. Med.* **355**, 1222–1232
8. Lunde, K., Solheim, S., Aakhus, S., Arnesen, H., Abdelnoor, M., Egeland, T., Endresen, K., Ilebekk, A., Mangschau, A., Fjeld, J.G., Smith, H.J., Taraldsrud, E., Grøgaard, H.K., Bjørnerheim, R., Brekke, M., Müller, C., Hopp, E., Ragnarsson, A., Brinchmann, J.E., and Forfang, K. (2006) Intracoronary injection of mononuclear bone marrow cells in acute myocardial infarction. *N. Engl. J. Med.* **355**, 1199–1209
9. Janssens, S., Dubois, C., Bogaert, J., Theunissen, K., Deroose, C., Desmet, W., Kalantzi, M., Herbots, L., Sinnaeve, P., Dens, J., Maertens, J., Rademakers, F., Dymarkowske, S., Gheysens, O., Cleemput, J.V., Bormans, G., Nuyts, J., Belmans, A., Mortelmans, L., Boogaerts, M., and Van de Werf, F. (2006) Autologous bone marrow-derived stem-cell transfer in patients with ST-segment elevation myocardial infarction: double-blind, randomised controlled trial. *Lancet* **367**, 113–121

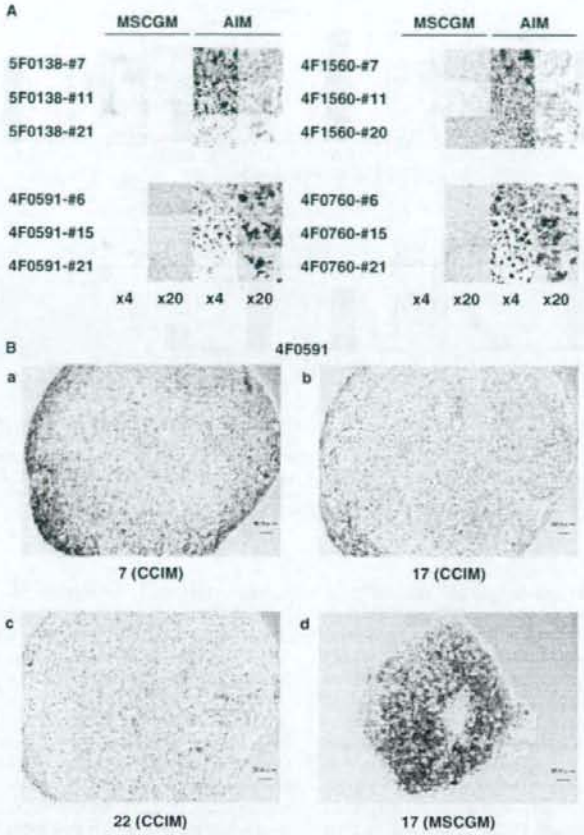

Fig. 3. **Adipogenic differentiation and chondrogenic differentiation of hMSCs.** (A) The cells in each passage numbers indicated were plated on 24-well plates and cultured in MSCGM (as control) or AIM (adipogenic differentiation medium) for 21 days. The cells were stained with Oil Red O. (B) The cells in passage. #7, #17 or #22 of 4F0591 were cultured in CCIM for 24 days and stained with Safranin O (a, b, c, respectively). Proteoglicans stained red. The cells in passage #17 were also cultured in MSCGM (as control) for 24 days (d).

interesting to investigate the gene expression profile of the 3D culture of hMSCs.

In conclusion, microarray and RT–PCR data of the six batches of hMSCs suggested that four genes, *EPHA5*, *NOV*, *NDN* and *RUNX2* have the potential to act as stage-specific markers during hMSC culture. These genes can be used as candidates for quality control markers of the culture status with regard to the differentiation potential for future clinical application of hMSCs for cellular therapeutics. We reported that the capacity of hMSCs for osteogenic differentiation was highly suppressed during the late culture stages. *NDN* or *RUNX2* may be a quality control marker of hMSC capacity for osteogenic differentiation. The observations of adipogenic differentiation of hMSCs suggested that each batch shows different transition in differentiation potential. It seemed that the capacity tends to be suppressed in late stage of the culture. The observations of chondrogenic differentiation suggested that the differentiation potential of hMSCs is retained in late stage of the culture. It seems that the cells in the late stage have limited differentiation potential (oligopotent). Furthermore, network analysis and gene expression analysis revealed that the expression profiles are distinct for each passage number. These findings imply the importance of quality control for safe application of hMSCs for cellular therapy and usefulness of expression analysis for finding marker genes. Phenotype profiling and profiling at the genome level, including chromosomal analysis, might need more research in the future. The profiling of the cells, in both differentiated and 3D states, will also need to be investigated for future clinical applications.

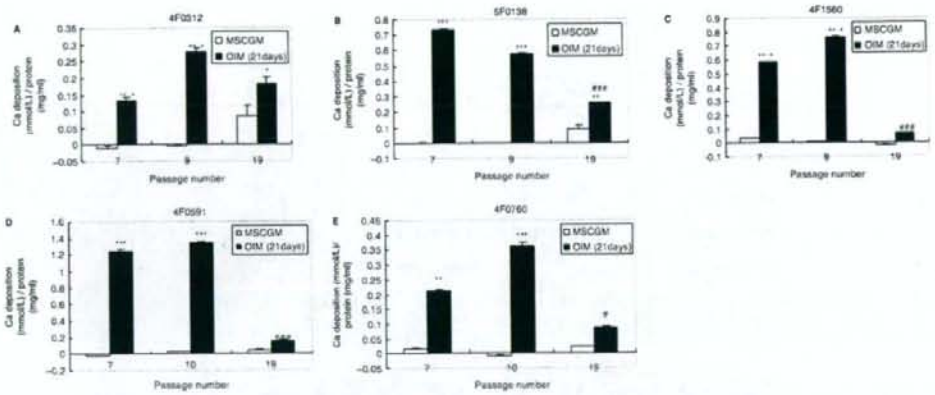

Fig. 2. **Calcium deposition of hMSCs.** The cells in each passage numbers indicated were plated on 12-well plates and cultured in MSCGM (control: clear column) or OIM (osteogenic differentiated; filled column) for 21 days. The amounts of calcium deposition in 4F0312, 5F0138, 4F1560, 4F0591 and 4F0760 are indicated in (A, B, C, D and E), respectively. Calcium deposition divided by protein concentration is showed as mean + SEM in triplicate. $^{***}P<0.001$, $^{**}P<0.01$, $^{*}P<0.05$ when osteogenesis in MSCGM was compared to that in OIM in each passage number. ### $P<0.001$, ## $P<0.01$, # $P<0.05$ when osteogenesis in passage #19 was compared to that in passage number 7 ($n=3$).

hMSCs through early and late stages of cell culture. Replication was performed by testing six different batches of cells. All six batches examined showed a marked decrease in culture growth rate with increasing passages.

The hMSC potential for osteogenic differentiation was down-regulated in all the batches of hMSCs examined during the late culture stage. The osteogenic differentiation was observed in all the batches of hMSCs examined for passages 7, 9 and 10. Also, every batch examined showed a down-regulation of the osteogeneic process during the 19th passage. As previously stated, four genes, *NDN*, *EPHA5*, *NOV* and *RUNX2* showed altered expression depending on the culture stage. *EPHA5* and *NOV* were up-regulated as the cells were further passaged, while *NDN* and *RUNX2* were down-regulated.

RT–PCR data indicated that the expression of *NDN* in all batches examined decreased during the late stages of culture. The expression of *NDN* in lot #4F1127, #4F0312 and #5F0138 was relatively stable until the 14th passage, which was then followed by a decrease in expression during the late stages. Microarray data also showed that the expression of *NDN* in passages 22–28 were decreased compared to that in passages 4–8. Furthermore, our results showed a positive correlation between the expression of *NDN* in hMSCs and the potential to differentiate into osteogenic cells as measured by the calcium deposition rates. Previous reports suggested that necdin, an *NDN* homolog, interacts with IL-1α precursor (*24*). The expression of *NDN* in hMSCs decreases with increasing passages. It is possible that *NDN* down-regulation is involved in activation of IL1-Myd88 pathway by dying cells (*25*).

Every batch showed a passage-dependent increase in the expression level of *EPHA5*. EPHA5 is transmembrane receptor protein tyrosine kinase, known as Ephrin A5 receptor, and belongs to the ephrin receptor subfamily. Recently, it has been shown that EPHA5 is involved in cellular growth and tumor malignancies (*26*, *27*). Also, it is known that the expression level of human *EPHA5* mRNA is high in primary human breast carcinoma cells (*28*).

NOV/CCN3 is a growth factor that plays several roles in cellular migration, growth, proliferation and chemotaxis. The previous finding that *NOV* inhibits the proliferation of a cancer cell line is consistent with the observation that *NOV* expression level is increased in the senescing phase, which coincides with the low proliferative stage of hMSCs. Furthermore, in primary skin fibroblasts, NOV/CCN3 protein increases the expression of human *SERPINE1* mRNA level (*29*). This is consistent with our observation that the expressions of *SERPINE1* as well as *NOV* are up-regulated during the late stages of cell culture. Mutant human SERPINE1 (T333R; A355R), which lacks the protease-inhibitory activity, decreases the quantity of rat laminin and inhibits matrix accumulation (*30*). On the other hand, previous finding indicated that the expression of mouse *Myod1* (myogenic differentiation 1) mRNA level and Myog (myogenin) protein decreased in C2/4 cells (subclone of C2C12 mesenchymal cells) stably expressing NOV, which suggests that NOV suppresses the myogenic differentiation of C2/4 cells (*31*).

The expression of *RUNX2* was also decreased in late stage of the culture. *RUNX2* is a member of the runt family of transcription factors and suggested to be involved in osteogenesis (*22*). It is possible that down-regulated osteogenic differentiation of hMSCs is caused by the decreased expression of *RUNX2*. Recent reports have shown that 3D cultures of human adipose tissue-derived endothelial and osteoblastic progenitors generate osteogenic–vasculogenic constructs (*32*). It might be

Table 1. **Continued.**

Analysis	Molecules in network	Score	Focus molecules	Top functions
5F0138-#9	ABCA1, AEBP1, ARG2, BGN, C1q, C1R, C1S, CYP2B6 (includes EG:1555), DDIT4, ENPP1, FABP5, FADS1, GDF15, HABP2, N-cor, NCOR-LXR-Oxysterol-RXR-9 cis RA, NFkB, Nr1h, OLR1, PCK2, PDGF BB, PTGDR, Rxr, SCD, SERPING1, SFTPD, SORBS3, SREBF1, SYNE1, THBS2, Thyroid hormone receptor, TNFAIP6, TNFSF9, TRIB3, VDR	46	27	Respiratory Disease, Inflammatory Disease, Lipid Metabolism
4F1127-#9	ACAN, Alkaline Phosphatase, Ap1, ASPN, C3, CCL2, CCNO, COL13A1, CP, FABP5, GEM, HMOX1, HOMER2, IGFBP5, IL1, JAG1, LDB3, LDL, Mmp, MMP28, NFkB, P38 MAPK, Pdgf, PDGF BB, RGS4, SERPINB2, SPINT2, SPP1, TAC1, Tgf beta, TNFAIP6, TNFRSF11B, TXNIP, VitaminD3-VDR-RXR, ZNF335	45	24	Cellular Development, Cellular Growth and Proliferation, Skeletal and Muscular System Development and Function
4F1127-#22	AEBP1, ANKRD1, C1q, C1R, CBR3, CD36, CFH, ENPP1, FLNC, FOXF1, G0S2, HAMP, HDL, HIST2H2AA3, HIST2H2BE, HIVEP1, IGKC, KCNAB1, KCND2, KRT17, LDB3, LY6E (includes EG:4061), MYOZ1, NFkB, OLR1, PLK3, POU2F2, REG3A, RIPK4, SLC40A1, TNFRSF19, TNFRSF10D, TNFSF9, TSLP, VSNL1	44	32	Genetic Disorder, Metabolic Disease, Molecular Transport
4F0760-#28	Alpha Actinin, CDH1, CTSH, Cyclin A, Cyclin E, E2f, EDN1, GAST, ICAM2, Integrin, ITGA2, ITGA6, KRT7, KRT18, LAMC2, MARCKSL1, Mek1/2, Mmp, MYOZ2, OCLN, PCOLCE, PCOLCE2, Plc beta, PLCB4, PRPS1, Rb, S100A4, SCG5, SDPR, SERPINB2, SMURF2, TFPI2, TGFB1, TNFRSF11B, TSPAN8	44	26	Cardiovascular System Development and Function, Cell Morphology, Skeletal and Muscular System Development and Function
4F0591-#7	AMELX, AQP4, ARNT2, BAT3, beta-estradiol, BIRC5, CATSPERB, CDCA8, CEBPA, CGREF1, DLGAP1, GLIPR1, GPR37, GRIN1, GTSE1, HSPA2, HSPA5, INS1, LITAF, NCAPG (includes EG:64151), NFkB, NPAS1, PLGLB2, RAB31, RAGE, retinoic acid, RPS14, RPS4X, RRM2, SCG2, STXBP4, TF, TGFBI, TP53, TRHDE	38	16	Cell Death, Cancer, Respiratory Disease
4F1127-#7	Actin, ADIPOQ, Akt, Ap1, BCL9, BIRC5, CCL2, CPE, EGR2, ERCC6L, HIST1H4C, Histone h3, HOMER2, IL1, IL8, Jnk, KRT18, LDL, NFkB, OSBP, P38 MAPK, PBK, PDGF BB, PDGFC, PLK1, POSTN, PRDX4, SERPINA3, SFRP4, SLC2A3, Tgf beta, TIFA, TNFRSF11B, TNFRSF1B, TPT1	35	17	Cellular Growth and Proliferation, Cellular Development, Hematological System Development and Function
5F0138-#7	Akt, Ap1, ASNS, CALM2, DAD1, DDIT4, FSTL1, G0S2, GARS, GDF15, HTRA1, JAK3, LDHA, LDL, LOX, MMP1 (includes EG:4312), NFkB, P38 MAPK, PCK2, PCOLCE, PDGF BB, PDGFC, PDPN, RND3, RPN2, SFRP1, SLC7A1, TCR, TGFB1, TIMP4, TNFRSF8, TNFSF9, TRIB3, UGDH, WNT2	30	15	Cancer, Cellular Movement, Cellular Development

The top networks in each analysis data analyzed by IPA are listed.

Table 1. **List of the networks in hMSCs.**

Analysis	Molecules in network	Score	Focus molecules	Top functions
4F0591-#9	BUB1B, CCNB1, CDC2, CDKN3, CENPF, CGREF1, Cyclin E, DLG7, E2f, ERCC6L, FOXM1, KRT8, LRP1, MAD2L1, MEOX2, NDC80, NFkB, NUF2, NUSAP1, OLR1, PBK, PCSK1, PLK1, PTTG1, RAD51AP1, Rb, RNA polymerase II, RRM2, SERPINB2, SPC25, TFPI2, TNFSF9, TRADD, TYMS, UBE2C	65	30	Cell Cycle, Cancer, Reproductive System Disease
4F1560-#28	ADH1B, ALDH1A3, BEX1 (includes EG:55859), BMP15, CD80, CHI3L1, DBP, DLX1, ENPP1, FGF5, GBP2, IGF2, Igfbp, IGFBP5, KRT19, LBP, MEOX2, Mmp, NFkB, NOV, PCSK1, PCSK5, PEG10, PYCARD, RAGE, SEPP1, SERPINB2, SERPING1, ST8SIA1, Tgf beta, TLR1, TNFAIP6, TNFSF15, TRAF4, TSLP	57	31	Cancer, Cellular Growth and Proliferation, Neurological Disease
4F0760-#9	ANKRD1, Ap1, BIRC3, CCNB1, CCR2, CDC2, CENPE, COL15A1, FBLN5, Jnk, LATS1, Mmp, MSR1, NDC80, NFkB, NRL, NUF2, OMD, PBK, Pdgf, PDGF BB, PDGFD, PRDM1, S100A4, SERPINB2, SLC37A4, SORBS3, SPC24, SPC25, TFPI2, THBD, TNFRSF8, VANGL2, VAV3, VSNL1	56	29	Cancer, Cell Cycle, Reproductive System Disease
5F0138-#24	ARLAC, BUB1 (includes EG:699), BUB1B, CCNB1, CCNB2, CCNF, CDC2, CDC7, CDC20, CDC25C, CDKN3, CENPE, CENPH, Cyclin B, Cyclin E, FBXO5, FOXM1, GINS1, GPNMB, IL6, KIAA0101, KIF11, KIF22, KIF2C, MRVI1, NDC80, NUF2, PBK, PLK4, PTTG1, SLC7A7, SPC25, UBE2C, VTCN1, ZWINT (includes EG:11130)	52	33	Cell Cycle, Cancer, DNA Replication, Recombination, and Repair
4F1560-#9	14-3-3, AURKA, BIRC5, CCNB1, CDC20, CDC25C, CDCA8, Cyclin B, Cyclin E, E2f, IGF2, MAD2L1, NDC80, NFkB, NUF2, OLR1, PBK, PRR11, RAD51AP1, Rb, RGS7, RNA polymerase II, RRM2, Scf, SERPINB2, SFN, SFRP4, SPC24, SPC25, TNFRSF8, TOP2A, TYMS, UBE2C, UHRF1, ZNF74	52	27	Cancer, Cell Cycle, Reproductive System Disease
4F0591-#28	AEBP1, ALDH1A3, ANGPT1, ANKRD1, BEX1 (includes EG:55859), C1R, CGREF1, CXCL16, DIRAS3, GAD1, HDAC9, ID4, IL1, IL1R1, KRT18, KRT19, MEOX2, Mmp, MYBL1, MYPN, NFkB, OLR1, PAK1IP1, Pdgf Ab, PLAT, PYCARD, RIPK4, SERPINB2, SERPINF1, SERPING1, TFPI2, Tgf beta, TNFRSF19, TNFRSF11B, TSLP	51	30	Cancer, Cardiovascular Disease, Cell Death
4F0312-#7	A2M, ACAN, ASPN, BRCA1, C1R, C1S, CEBPD, CYP27A1, DDIT3, DDIT4, ESR1, FGF7, GDF15, IL1, Jnk, KSR2, MAD2L1, Mek, Mek1/2, Mmp, NFkB, NOTCH3, NOX4, NR4A1, OSMR, P38 MAPK, PCK2, Pdgf, PDGF BB, SERPINB2, STAT, TNFAIP6, TNFSF9, TNFSF15, TRIB3	50	25	Cell Cycle, Inflammatory Disease, Cellular Development
4F0312-#28	ANKRD1, BEX1 (includes EG:55859), BLK, CD36, CDKN2B, CTSL2, ENPP1, F2RL1, FABP5, FKBP5, FUS, G0S2, GAD1, GDF15, IGFBP5, IGHG1, IL1, N-cor, NFkB, OLR1, PAPPA2, PLAT, PNRC1, Rxr, RXRA, SERPINB2, STMN2, Tgf beta, THRB, Thyroid hormone receptor, TNFRSF19, TNFRSF11B, TNFSF13B, TRIP13, VSNL1	50	29	Cancer, Cellular Growth and Proliferation, Immunological Disease
4F1560-#7	14-3-3, AURKA, BIRC5, CCNE2 (includes EG:9134), CDC25A, CDCA8, CEBPA, CENPF, CSPG4, Cyclin A, Cyclin E, E2f, ESPL1, FEN1, FMOD, Histone h3, Mapk, MCM8, MCM10, MDM4, NUSAP1, OIP5, PP2A, PRR11, PTTG1, Rb, RGS7, RRM2, SFRP4, SMPDL3A, SOS2, TOP2A, TTK, TYMS, UBE2C	50	27	Cell Cycle, Cancer, Reproductive System Disease
4F0312-#9	ABCA1, ACAN, AEBP1, Akt, ANXA11, ASPN, C1R, C1S, CD36, DKK, F2RL1, FBLN1, FGF7, FOXE1, GDA, GDF15, HSD11B1, IGF2, IGFBP2, Insulin, LDL, LEPR, Mapk, NFkB, NTF3, P38 MAPK, PDGF BB, PTX3, SLC7A7, THBS2, TNFAIP6, TNFSF9, Wnt, WNT2, WNT16	49	23	Lipid Metabolism, Molecular Transport, Small Molecule Biochemistry

(continued)

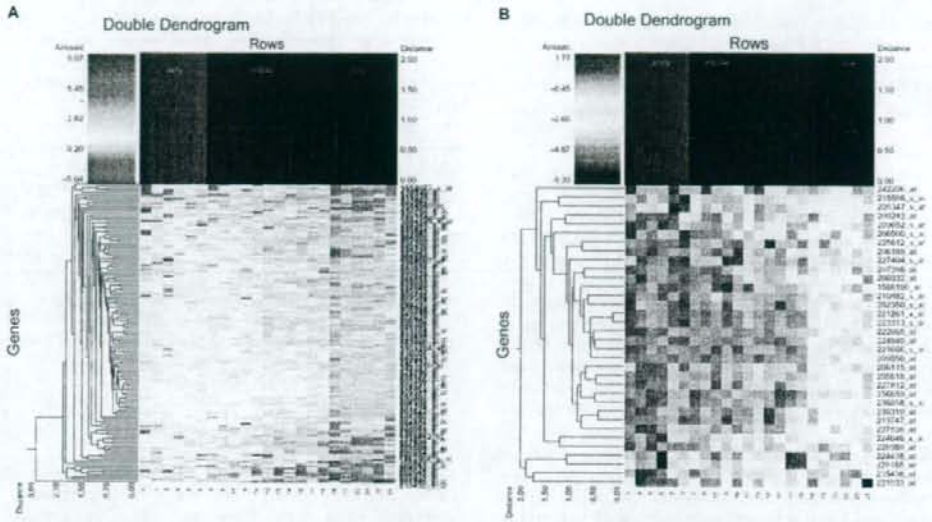

Fig. 1. **Microarray analysis of hMSCs.** One hundred and sixty-nine probe sets extracted from microarray data of six batches of hMSCs. [$n = 6$ in early stage (#4 or 5), passage #9, late stage (#22, 24 or 28), $n = 5$ in passage #7]. Cut off value of signal intensity ratio (max/min of average in each stage) is 2.949145023 [5% change in each passage number from early to late stage; $1.05^{(\text{passage number range of average in early and late stage})}$]. Double dendrograms of up-regulated 135 probe sets (A) and down-regulated 34 probe sets (B) are shown.

stages of cell culture. These findings suggest that the expression levels of genes associated with osteogenesis are different at the late stages compared with those at earlier stages of cell culture.

Statistical analysis of microarray and calcium deposition data from three batches (5F0138, 4F1560, 4F0591) of hMSCs in middle (#7–10) and late (#19–28) stages showed that the expression of *NDN* [necdin homolog (mouse)] has a positive correlation with calcium deposition ($P < 0.05$).

Adipogenic Differentiation of hMSCs—Figure 3A shows the results of Oil Red O staining of adipogenic-induced cells. The cells were adipogenic induced for 21 days and lipid was stained with Oil Red O. Adipogenesis of hMSCs seemed to be down-regulated in late culture stage of 5F0138, 4F0591 and 4F0760, while the adipogenic-differentiation capacity seemed to be retained in passage #20 of 4F1560.

Chondrogenic Differentiaion of hMSCs—Figure 3B shows the Safranin-O staining of chondrogenine-differentiated hMSCs. The cells were differentiated in CCIM for 24 days and stained with Safranin-O. The culture in passages 7, 17 and 22 of 4F0591 showed chondrogenic-differentiated morphology (a, b, c, respectively). The culture in late stage seemed to be chondrogenic differentiated as shown (c). The cells cultured in MSCGM as control did not show any chondrogenic-differentiated morphology (d).

RT–PCR Analysis of hMSCs—The quantitative RT–PCR data showed that some genes had similar expression profiles in all the six batches examined. Up-regulated genes, which were identified as candidates for the stage-specific markers included *EPHA5* (EPH receptor A5), *NOV* (nephroblastoma overexpressed gene), *SERPINE1* [serpin peptidase inhibitor clade E (nexin, plasminogen activator inhibitor type 1), member 1], *ITGA4* [integrin, alpha 4 (antigen CD49D, alpha 4 subunit of VLA-4 receptor)], and down-regulated genes, which are also candidates for the stage-specific markers included *NDN*, *RUNX2* (runt-related transcription factor 2) and *RUNX3* (runt-related transcription factor 3). *NOV* is a growth factor and is involved in the proliferation of bone cancer cell lines (*20*). It is notable that the expression of *NOV* in lot #4F1127 was relatively stable. *SERPINE1* is involved in the protein-binding function and diseases such as heart failure (*21*). *RUNX2* is a member of the runt domain-containing family of transcription factors and suggested to regulate osteogenic differentiation (*22*). *RUNX3* is also a member of the runt domain-containing family of transcription factors and a candidate tumor suppressor (*23*). *EPHA5*, *NOV*, *NDN* and *RUNX2* showed altered expression correlating with passage numbers ($P < 0.01$) (Fig. 4). The results of RT–PCR analysis of 45 genes examined are shown in Supplementary Fig. 2.

DISCUSSION

hMSCs will be used for cellular therapeutics in clinical settings in the near future. The importance of quality control of the cells will be significant as the use of cellular therapeutics becomes more common. In this report, we report on profiling the gene expression of

Cluster Analysis—The microarray data of 169 probe sets obtained from six batches of hMSCs was subject to cluster analysis using the Gene Expression Statistical System (NCSS, Kaysville, Utah; Dr Jerry L. Hintze). Fold change of signal intensity to the average signal intensity of early stage was analysed and a double dendrogram was plotted on a log 2 scale.

Gene Ontology Analysis—Gene ontology analysis was conducted using Ingenuity Pathway Analysis (IPA) (Ingenuity® Systems, Redwood City, California, USA), NetAffyx (Affymetrix) and GOTM (Gene Ontology Tree Machine, Vanderbilt University, Nashville, Tennessee, USA) analyses. Probe sets with signal intensity values associated with the passage numbers were subject to analyses. The functional analysis identified the biological function and/or diseases that were most significant to the data set. Genes from the data set that were associated with biological functions and/or diseases in the Ingenuity Pathways Knowledge Base (IPKB) were considered for further analysis.

cDNA Synthesis and Real-time PCR Using Taqman Low-density Array—RT–PCR (reverse transcriptase–PCR) analysis was performed to assess the mRNA levels in six batches of hMSCs using TaqMan® low-density array (TLDA) (Format 48) (Applied Biosystems, Foster City, California, USA). The data was normalized using *GAPDH* (glyceraldehyde-3-phosphate dehydrogenase). Forty-six genes including *GAPDH* as endogenous control are listed in Supplementary Table 1. cDNA was synthesized using a High-capacity cDNA synthesis kit (Applied Biosystems) and Multiscribe reverse transcriptase. cDNA synthesized from 100 ng of total RNA was used for the analysis (2 ng of total RNA per well). Real-time PCR was analysed using 7900 HT real-time PCR system (Applied Biosystems). The conditions for the PCR reaction were as follows: 50°C (2 min) and 94.5°C (10 min), and 40 cycles at 97°C (30 sec) and 59.7°C (1 min). Relative quantification values were calculated by the comparative Ct method using SDS 2.2.2 software (Applied Biosystems).

Pathway Network Analysis—Data were analysed using the IPA (Ingenuity® Systems, www.ingenuity.com). A data set containing gene identifiers and corresponding expression values was uploaded into the application. Each gene identifier was mapped to its corresponding gene object in the IPKB. A fold-change cutoff of 3 for both up- and down-regulation and a p-value cutoff of 0.05 were set to identify the genes to be analysed. These genes, called focus molecules, were overlaid onto a global molecular network developed from information in the IPKB. Networks of these focus molecules were then algorithmically generated based on their connectivity. The functional analysis of a network identified the biological functions and/or diseases that were most significant to the genes in the network. The genes in the networks associated with biological functions and/or diseases in the IPKB were considered for the analysis. Genes and gene products are represented as nodes, and the biological relationship between two nodes is represented as an edge (line). All edges are supported by at least one reference from the literature, textbook or canonical information stored in the IPKB. Human, mouse and rat orthologs of a gene are stored as separate objects in the IPKB, but are represented as a single node in the network. The node colour indicates the degree of up- (red) or down- (green) regulation. Nodes are displayed using various shapes that represent the functional class of the gene product.

Statistical Analyses—Non-parametric analysis was used for microarray data analyses. The Spearman correlation coefficient and two-tailed p-values were calculated. $P < 0.001$ or $P < 0.05$ were considered to be significant. RT–PCR data was analysed with non-parametric analysis. The Spearman correlation coefficient and two-tailed p-values were calculated. To compare the specific passage number and stage, Student's t test was performed. Two-way ANOVA followed by Bonferroni post-test was performed for osteogenesis data. GraphPad Prism® 4 and Microsoft® Office Excel were used for statistical analysis and drawing graphs.

RESULTS

Microarray Analysis of hMSCs—To identify the quality-control markers in different stage of the culture, we performed DNA microarray analyses. Non-parametric analysis and a ratio (max/min of signal intensity) cutoff of 3.071,524 ($1.05^{(28-5)}$; 5% change in each passage from 5th to 28th) showed that the expression level of 341 probe sets out of a total of 54,613 probe sets had a significant association with passage numbers (hMSC lot #4F1560, passage numbers 5, 7, 9, 13, 21 and 28).

Gene ontology analyses showed that the mapped genes corresponded to the probe sets belonging to various categories of molecular and cellular functions such as cell-to-cell signaling and interaction, cellular movement, cell death, cellular assembly, cellular organization and cell cycle, and physiological system development, and biological functions such as hematological system development and function, immune and lymphatic system development and function, tissue development, immune response and embryonic development. The top five disease categories that the genes mapped to, as identified using the IPA software, included cardiovascular, hematological, musculoskeletal, oncogenic and reproductive disorders.

Figure 1 shows the results of cluster analysis obtained from microarray data of six batches of hMSCs in early (passage #4–5), middle (#7–9) and late stages (#22–28). Seventy-nine genes out of the 169 probe sets were categorized by function and disease as per IPA analysis. Networks were analysed for each of the six batches and a representative network is shown in the Supplementary Fig. 1. A list of all top networks in each analysis is shown in Table 1. Many network categories with the top score in each analysis were involved in cancer or regulation of cell cycle. Additionally, specific networks for each sample were generated when the batches were individually analysed.

Calcium Deposition of Osteogenic-induced Cells—In Fig. 2, calcium deposition in hMSC cultures (4F0312, 5F0138, 4F1560, 4F0591, 4F0760) were measured during passages 7, 9, 10 and 19. The results showed that the osteogenic differentiation occurred in early to middle stages and was dramatically suppressed during the late